A 100 kHz Pulse Shaping 2D-IR Spectrometer Based On Dual Yb:KGW Amplifiers

P.M. DONALDSON,[1]* G.M. GREETHAM,[1] D.J. SHAW,[1,2] A.W. PARKER[1]

AND M. TOWRIE[1]

[1] *Central Laser Facility, Science and Technology Facilities Council, Research Complex at Harwell, Rutherford Appleton Laboratory, Didcot, OX11 0QX, UK*
[2] *Department of Physics, University of Strathclyde, SUPA, 107 Rottenrow East, Glasgow, G4 0NG, UK (Present address: UCB Pharma, Structural Biology, Slough, SL1 3WE, UK)*

*Corresponding author: paul.donaldson@stfc.ac.uk

A high-speed, high-sensitivity and compact two dimensional infrared (2D-IR) spectrometer based on 100 kHz Yb:KGW regenerative amplifier technology is described and demonstrated. The setup is three colour, using an independent pump OPA and two separately tuneable probe OPAs. The spectrometer uses 100 kHz acousto-optic pulse shaping on the pump beam for rapid 2D-IR acquisitions. The shot-to-shot stability of the laser system yields excellent signal-to-noise figures (~10 μOD noise on 5000 laser shots). We show that the reduced bandwidth of the Yb:KGW amplifiers in comparison with conventional Ti:Sapphire systems does not compromise the ability of the setup to generate high quality 2D-IR data. Instrument responses of < 300 fs are demonstrated and 2D-IR data presented for several systems of interest to physical chemists, showing spectral diffusion in NaSCN, amide I and II bands of a beta sheet protein and DNA base-pair – backbone couplings. Overall, the increased data acquisition speed, intrinsic stability and robustness of the Yb:KGW lasers are a significant step forward for 2D-IR spectroscopy.

Introduction

Infrared (IR) spectroscopy in its many forms is established as a useful tool across the physical and life sciences. Ultrafast Two Dimensional Infrared (2D-IR) spectroscopy is a significant enhancement of conventional IR absorption spectroscopy, as it reveals equilibrium structural dynamics, vibrational mode coupling and energy transfer. 2D-IR spectroscopy employs IR laser pulses that are of a shorter / similar duration to the vibrational dephasing and population relaxation times of the system of interest. In various arrangements of excitation and probing pulses,[1] 2D-IR spectroscopy provides a unique means to understand the fundamental properties that relate structure and molecular interactions and how these influence the chemistry underpinning biological processes, offering a new window into hydrogen bond dynamics,[2] proton dynamics,[3] chemical exchange processes,[4,5] fibril formation,[6] protein secondary structure determination[7] and enzyme active site dynamics[8,9] to name a few.

For 2D-IR spectroscopy to reach its full potential, the operation of 2D-IR spectrometers needs to improve on many fronts. In particular, signal-to-noise, data acquisition speed, tunability of the IR laser beams, ease /

robustness of operation, the complexity of the setup and the cost of ownership are all areas that make 2D-IR spectroscopy to-date a relatively niche method. Since the first measurements of ultrafast 2D-IR spectra,[10] many technical developments in spectrometer design have become available to improve on the speed, sensitivity and reliability of acquisition of 2D-IR data.[11-20] The other significant area where improvement is required is in the laser sources used. So far, most published 2D-IR setups have used IR light generated through nonlinear processes driven by commercial Ti:Sapphire amplifiers. Whilst a mature technology, the drawbacks of Ti:Sapphire amplifiers are their large footprint multiple-unit lasers with a high degree of user competence required to maintain consistent output over the laser's lifespan. Meanwhile the scalability of Ti:Sapphire amplifiers in terms of power and/or repetition rate is limited.

To-date, Ti:Sapphire based 2D-IR setups reported in the literature typically operate at 1-10 kHz repetition rates. Amplifier systems operating at 100 kHz have been in existence for several decades, and although useful for transient visible spectroscopy,[21] they do not develop enough power to be converted to infrared light of sufficient intensity for practical spectroscopy. In an earlier work,[22] we demonstrated a customized, commercially available, Yb:KGW regenerative amplifier system for time-resolved infrared (TR-IR) spectroscopy via 100 kHz IR probing and adjustable 1 Hz – 50 kHz repetition rate pumping. The diode-pumped solid-state design of this Yb:KGW amplifier technology provides efficiency and robust performance at this high repetition rate, with a small size, high stability, high reliability and low maintenance overheads. Similar Yb:KGW laser technology has been used advantageously elsewhere with non-collinear OPAs for broadband impulsive Raman spectroscopy,[23] and recently for 2D electronic spectroscopy,[24] which can be usefully compared with recent lower repetition rate developments.[25] In this paper, we demonstrate how Yb:KGW regenerative amplifiers can be used for 2D-IR spectroscopy at 100 kHz repetition rate. Yb:KGW lasers generate 2-3x longer pulses than Ti:Sapphire systems, raising the practical question of whether this is enough bandwidth/time resolution to be useful. We address these issues in this paper by showing that the bandwidth is sufficient to cover a large number of bands of interest in DNA and proteins and that the time resolution is sufficient for capturing the spectral diffusion on sub-picosecond timescales, illustrated via centre-line-slope (CLS) 2D-IR measurements of SCN^- in H_2O.

2D-IR spectroscopy was recently demonstrated at 100 kHz using a home-built, 220 fs pulse duration IR Optical Parametric Chirped Pulse Amplification (OPCPA) system.[26,27] To date however there is little data on signal-to-noise, detection limits and IR tunability to compare OPCPA 2D-IR setups with the OPA 2D-IR data presented in the current paper. Nevertheless, OPCPA is a highly promising technology that has recently become available commercially, with mid-IR signal/idler beams of energies of tens of μJ/pulse at hundreds of kHz, and <100 fs pulse durations typical.[28] At the time of writing, OPCPA systems are less well developed than the Yb:KGW / OPA technology used here, but will undoubtedly produce tunable light with greater bandwidth and temporal flexibility– perhaps at the expense of extra operational complexity. Yb:KGW regenerative amplifier and OPA technology is also still developing in terms of performance offered. We thus believe that commercial Yb:KGW / OPA systems such as the one described in this paper currently offers a simple, robust route to 100 kHz 2D-IR spectroscopy, especially to the spectroscopist who does not always wish to concern themselves with the practicalities of correctly generating and characterising the IR light required for experiments.

For a given pulse energy, 100 kHz repetition rate 2D-IR spectroscopy will obviously give an improvement of between 3.3 to 10 times in signal-to-noise over typical 1-10 kHz sources. It is also worth noting that when signal-to-noise is not a concern (i.e. when samples of interest give strong signals), a 100 kHz source will straightforwardly accumulate data 10-100x faster – a highly relevant increase when acquisitions at lower repetition rates typically take minutes or tens of minutes. Noise in a Fourier transform measurement is also

typically not distributed equally at all frequencies and it is well known that over the same time frame, multiple faster acquisitions achieve higher signal-to-noise than a single, slower acquisition.[12,29] To achieve this advantage fully for 2D-IR measurements at 100 kHz, a pulse shaper-based 2D-IR spectrometer[11] is currently the only means of modulating the spectral amplitude and phase to generate on a shot by shot basis controllable delay phase cycled pulse pairs at 100 kHz for the resolution of the pump axis. Other 2D-IR methods require slower mechanical motion to change the delays and phases of the beams. We note that Yb:KGW regenerative amplifiers also allow access to high average power at high repetition rates - up to MHz.
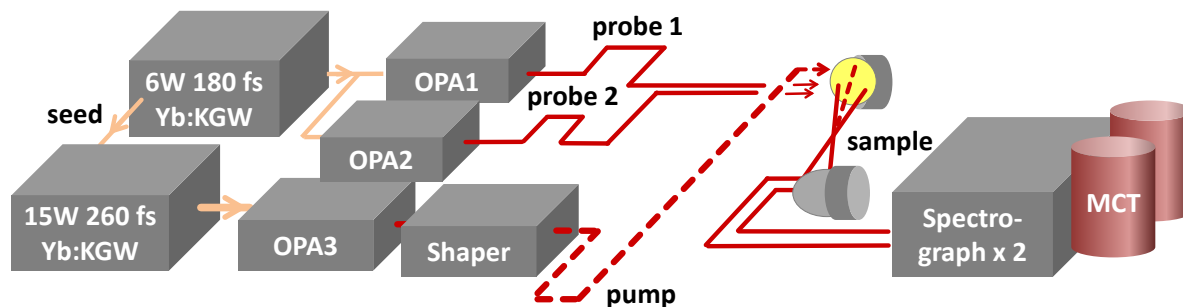

Fig. 1. Layout of the 100 kHz laser system and 2D-IR spectrometer

Methods

The 100 kHz 2D-IR spectrometer described in this paper, depicted in Figure 1 and is built around a customized dual Yb:KGW 1032 nm amplifier system (6 W Pharos-SP and 15 W Pharos, Light Conversion). For optical synchronization, a single oscillator in the 6 W Pharos unit seeds both regenerative amplifiers. The 6 W amplifier operates with a pulse duration of 180 fs and drives two optical parametric amplifiers (OPAs) that are used to generate separately wavelength tunable probe pulses. The 15 W amplifier system has a pulse duration of 260 fs and drives a single OPA that generates the wavelength tunable pump pulses. A more compact and economical 2D-IR setup could comprise a single regenerative amplifier driving one or two OPAs. The choice of customized dual amplifier – triple OPA configuration is based on the design aim of high pump energy for highest 2D-IR signal-to-noise, high probing bandwidth and the in-tandem use of the system to perform transient UV/Vis - IR spectroscopy with fs to μs pump-probe delays, and multiple probe pulses between each pump pulse – allowing for longer time kinetics.[22]

The OPAs in Figure 1 are configured as follows: The 6 W amplifier output is 50/50 split to pump two OPAs (Light Conversion Orpheus-One) that generate two probe beams. These OPAs are white light continuum (WLC) seeded, with a 515 nm pumped BBO pre-amplification, 1032 nm pumped KTA main amplification stages and final signal and idler DFG (Difference Frequency Generation) in gallium selenide (GaSe). This DFG output is tunable from 4.5 - 15 μm with typical pulse energies 0.2 to 0.3 μJ. The 15 W amplifier pumps a single OPA (Orpheus-HP) similar to above, but with an additional 515 nm pumped BBO amplification stage. Pulse energies in the λ = 4.5 to 10 μm part of the spectrum from this higher energy pump OPA are between 1.7 to 0.7 μJ. For both types of OPAs, at below 4.5 μm, the KTA generated idler can be used directly, and pulse energies increase by x3-4 compared with the peak values obtained by GaSe DFG.

It is worth noting that the 1032 nm pumped final OPA stages used here generate signal and idler at longer wavelengths than those from a Ti:Sapphire 800 nm pumped OPA. This longer wavelength can be advantageous in terms of reduced optical damage and thermal lensing effects in typical mid-IR generating

DFG materials such as GaSe and $AgGaS_2$. To minimize these, it is important to avoid the 2-photon absorption edges in such materials, typically in the visible/NIR part of the spectrum. Therefore, higher power mid-IR outputs are more accessible at the Yb:KGW 1032 nm pump wavelength relative to that of Ti:Sapphire (800 nm). Despite considerable thermal loading in the OPAs (e.g. tightly focused, 2-3 W signal + idler), the beam quality is excellent and after heavy use, the GaSe crystals show no sign of damage.

After exiting the OPA units, the two probe IR outputs are collimated to a waist of ~ 5 to 7 mm and delivered along matched path-lengths to opposite edges of an off-axis parabolic mirror (EFL 7.5 cm), giving focused spot sizes at the sample position of 50 to 75 μm full width half-maximum (FWHM). The probe beams are then recollimated with a second off-axis parabolic mirror and sent to two simple home-built imaging spectrographs, each comprising a grating, a 15 cm EFL curved mirror and a 128 element HgCdTe (MCT) array (IR Associates). The spectra acquired by each MCT detector are digitized at 100 kHz by an FPAS system (Infrared Systems Development Corporation). Originally specified for < 10 kHz operation, optimization of the acquisition subroutines allowed a single PC to acquire 100 kHz realtime spectra from 4 parallel detection systems between 80 and 144 elements.[22] The availability of two separate probe MCT array detectors also permits the simultaneous measurement of <xxxx> and <yyxx> 2D-IR signals. This is achieved by using a single probe beam polarized with a wire grid polarizer at 45 degrees relative to the pump beam. The probe light can then be split into parallel and perpendicular components, which are then routed to the separate detectors.

The pump OPA output is collimated to a waist of 4 mm and passes through a commercial 100 kHz acousto-optic pulse shaper based on a zero-dispersion 4f stretcher-compressor geometry (Phasetech Spectroscopy). Depending on wavelength and alignment, the shaper was measured to be 30-60% efficient (diffracted power out vs input power, gratings 150 lines/mm – Richardson 33009FL01-880R). The shaped output then passes over a computer-controlled delay stage for population time scanning. An extra fixed 2.5 m path-length over multiple mirrors was required to synchronize the pump with the probe beams. In future this delay could instead be added to the oscillator beam seeding the 15 W regenerative amplifier, reducing the IR losses over multiple mirrors and increasing the pump pulse energy (and therefore the 2D-IR signal) at the sample by 30%. Typically, at a 6 μm pump wavelength, with 1 μJ pulse exiting the OPA, a pulse energy of 0.2 μJ was incident on a sample (full diffracted output of shaper). Astigmatism introduced by the pulse shaper gave the focused pump beam a larger waist compared with the probe beams, pinhole transmission measurements indicating a spot size of ~ 100 μm FWHM. All samples were contained in commercial IR cells (Harrick) using 2mm thick CaF_2 windows and 50 μm pathlengths.

2D-IR spectroscopy was implemented in the pump-probe geometry, with pump pulse-pair coherence time scans carried out using acousto-optic pulse shaping.[30] Shaper waveforms were updated at 100 kHz, with each sequence of digitized IR probe measurements tagged by an accompanying synchronization pulse to identify the first pump waveform of the sequence. Phase cycling (typically four phases[1]) was used for lossless signal recovery and scatter suppression. In order to express the Fourier transformed 2D-IR signal amplitude in units that can be usefully compared between different instruments, different sample types and different measurement parameters (e.g. chopping, 2-4 frame phase cycling and different spectral resolutions), we do the following: the 2D-IR signal amplitude is normalized by the ratio of the amplitude of the pump-probe spectrum calculated by projection of the 2D-IR spectrum along the pump axis, to the amplitude of the pump-probe spectrum measured at zero coherence time by chopping or phase cycling (from the data prior to Fourier transforming). This gives a robust measure of 2D-IR signal size when collected in the pump-probe geometry. To make explicit this correction, we use the unit definition 'mOD norm'.

Results

Laser stability, bandwidths and instrument response. A critical part of any 2D-IR or TR-IR experiment is the accuracy in which probe spectral intensity differences can be measured. This accuracy depends on both the stability of the light source, the specific detectivity of the light sensing elements and the noise added upon signal integration and digitization. We describe in greater detail the characteristics of the 100 kHz detector electronics, data acquisition system and noise in reference 22. In brief we find that using the Yb:KGW driven OPAs as IR light sources, signal fidelity in the setup is limited by detector noise, not laser noise, and referencing by detecting an additional replica of the probe is therefore not necessary. Over 1s, (10^5 laser shots), the r.m.s noise in the measured mid-IR intensity is *c.* 0.15%. The standard deviation caused by noise on the difference of successive pairs of shots is, in absorbance units (i.e. *log (I_n/I_{n+1})*), observed to be around 0.5 mOD. For an averaged number of measurements *N,* this noise scales as $1/\sqrt{N}$. In accordance, a peak-to-peak, a noise of ~10 μOD is typically observed in the probe spectrum after an average of 5000 laser shots (50 ms). This is comparable in performance to well optimized 1-10 kHz Ti:Sapphire based setups,[12] but in one tenth to one hundredth of the acquisition time. To achieve this same level of signal-to-noise with Ti:Sapphire based setups, referencing[1] and careful OPA alignment[31] is often necessary. The 100 kHz Yb:KGW – OPA systems achieve their level of performance with less complexity and a much higher degree of long term stability.

Having established that the Yb:KGW based IR source presented here is, on a shot-to-shot basis, typically more stable than Ti:Sapphire-based IR sources, the remaining issue for Yb:KGW amplifier-based 2D-IR spectroscopy is whether the reduced bandwidth / increased pulse duration is practical to use for a sufficient number of chemical systems of interest. Figure 2(a) shows the pump and probe spectral intensities centered at 1650 cm^{-1} measured by the MCT array spectrometers of Figure 1. The FWHM probe bandwidth is 160 cm^{-1} and the pump bandwidth 80 cm^{-1}. These values are greater than those of the 1032 nm pump lasers, which are 127 and 67 cm^{-1} respectively. This increase in bandwidth is thought to occur via both the amplification of the white light to generate the signal seed (which for the probe OPA is non-collinear), and via the wide gain bandwidth of the KTA OPA and GaSe DFG processes.
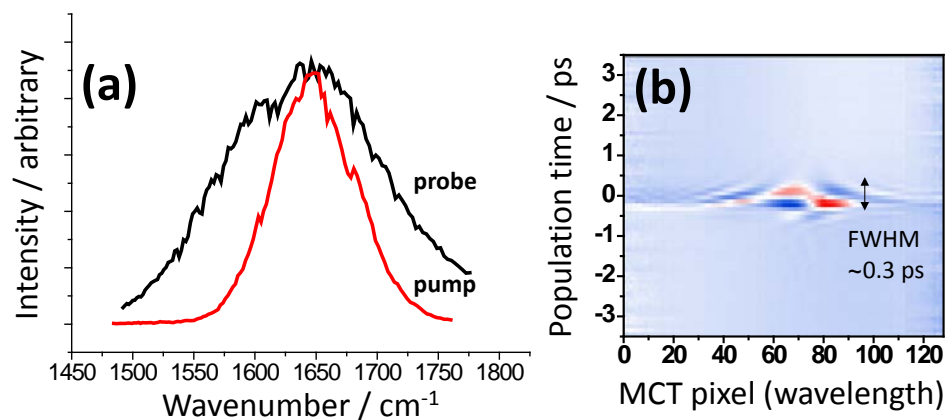

Fig. 2. (a) Dispersed spectral intensity of pump (red) and probe (black) measured on 128 pixel MCT arrays. (b) Non-resonant pump-probe Kerr response (CaF$_2$ windows) as a function of wavelength (MCT pixel).

Instrument response, important to 2D-IR spectroscopy measurements, can be conveniently observed in a pump-probe geometry via the dispersed, non-resonant Kerr response of the sample cell windows, or for the present laser system, also via the pump-probe response of a process faster than the pulse durations used, such as vibrational relaxation of H_2O. Figure 2(b) shows an example single-colour response measurement of the 2D-IR setup from a 2 mm thick piece of CaF_2. Although Kerr responses changes sign as a function of wavelength and waiting time, we find that integrating the absolute value of the response across the probe axis gives as a function of waiting time approximately Gaussian profiles which are then readily fit to provide a useful instrument response metric. The metric combines the slope of the response (showing the probe chirp) and the vertical width of the response (showing the pump chirp) – both of which should be minimised. This is achieved by systematically varying the group velocity dispersion (GVD) and third order dispersion (TOD) added to the pump beam by the pulse shaper mask and to the probe by addition or exchange of IR transmissive glasses.[32] Using the metric defined above, we observe 2D-IR instrument responses of 250-300 fs FWHM (tested across a 3-10 μm spectral range). This is reasonable given the spectral bandwidths of the pump and probe, which suggest transform-limited pulse durations of 180 and 90 fs, permitting an instrument response of not better than 200 fs. The lack of slope in Figure 2(b) indicates that the response is limited by the pump beam and could perhaps be improved using additional algorithms in the pulse shaping for correction of Bragg angle variation.[33] Identical FWHM values for response duration were determined separately by nonlinear autocorrelations of the shaped pump pulse and cross-correlations of the pump and probe by second harmonic generation (SHG) in $AgGaS_2$. We note that due to differences in GVD/TOD, for CaF_2 sample cells, the optimum pulse shaper dispersion corrections for best instrument response differ compared with that required for SHG in $AgGaS_2$.

2D-IR spectra I. Signal size, FFCF analysis and kinetics. N-methyl acetamide (NMA) is a model amide system that is useful as a standard for checking 2D-IR signal size during instrument setup. Figure 3 (a) and 3(b) show 2D-IR spectra of 100 mM NMA dissolved in D_2O for different two population times. Each spectrum was acquired in 1 second. The shape of early time spectra is visually identical to data published eslewhere.[34] The peak-to-peak amplitude of the chopped pump-probe signal from the 100 mM NMA-d was 20-30 mOD (50 μm pathlength, population time T_2=0.2 ps). This amplitude is comparable, if not slightly larger than that observed with 50 fs, 10 kHz[35] and 100 fs, 1 kHz[36] Ti:Sapphire based pump-probe setups. In both cases, these examples use 1.5 - 2 μJ of 6 μm mid-IR light generated from OPAs pumped with 500 μJ / pulse of 800 nm light. Although in principle, higher pulse energies are possible at this wavelength, in practice it is hard to achieve > 4-5 μJ without distortion from thermal lensing and accumulation of damage in the $AgGaS_2$ crystals used. The pulse energy at 6 μm from the Yb:KGW pumped OPA via KTA/GaSe was 1 μJ, which is 1.5-2x lower than the Ti:Sapphire sources compared here. In addition to pulse energy, the other factors to take into account regarding 2D-IR signal size are the significant dependence on pump-probe focusing/overlap, which we assume are similar in the cases compared here, and on the efficiency by which light can be delivered to the sample, which could be between 30 and 60% depending on the setup, purge conditions etc. Therefore, despite the 20% efficiency in delivering light to the sample for the Yb:KGW system, and lower overall source pulse energy, the fact that the pump-probe signal sizes from the NMA standard sample are comparable between the different setups indicates that the signal is increased by the narrower bandwidth and therefore higher spectral brightness of the Yb:KGW OPA pump pulses.

A common application of 2D-IR spectroscopy is to relate the slope, or ellipticity of a diagonal band 2D-IR spectrum as a function of population time to the frequency-frequency correlation function (FFCF).[1] As this involves the measurement of multiple 2D-IR spectra, there are significant benefits in conducting these measurements at the higher speed afforded by a 100 kHz 2D-IR setup, for example if multiple temperatures are required for Arrhenius analysis, or if very small differences in slope decay and offset are to be

distinguished. We note that when using a pulse shaper for FFCF measurements, it is especially important to ensure that the diffracted power out of the shaper is linear with drive amplitude. The drive amplitude at which the diffracted output begins to saturate varies with wavelength and with shaper alignment. A consequence of shaper output nonlinearity is the appearance of near-diagonal distortions in the 2D-IR spectra at early times that vary as a function of waiting time, making FFCF analysis difficult.

Figure 3(c) and 3(d) shows an early and a late-time 2D-IR spectrum of room temperature NaSCN dissolved in H_2O. The centre-line slope derived FFCC is shown in Figure 3(e) and comprises 23 2D-IR spectra, each averaged for 10 s, though the earlier times could have easily been acquired in < 1s. The slope exponential decay is 0.8 ps and in excellent agreement with earlier studies.[37] Likewise, at higher temperatures, we see the observed CLS decay time constant decrease, following Arrhenius-like behavior. We did not explore the limit at which the CLS decay becomes obscured by the instrument response, however at 365 K, CLS exponential decay fits with a decay time of 0.4 ps were reliably returned, still closely following Arrhenius kinetics. This provides a firm lower limit on the timescales observable with the Yb:KGW-pumped OPAs. Figure 3(e) also shows the decay of the bleach / excited state of the same 2D-IR spectra used for the CLS analysis as a function of waiting time. The smoothness of the decays clearly demonstrate the high degree of stability in the pump beam.
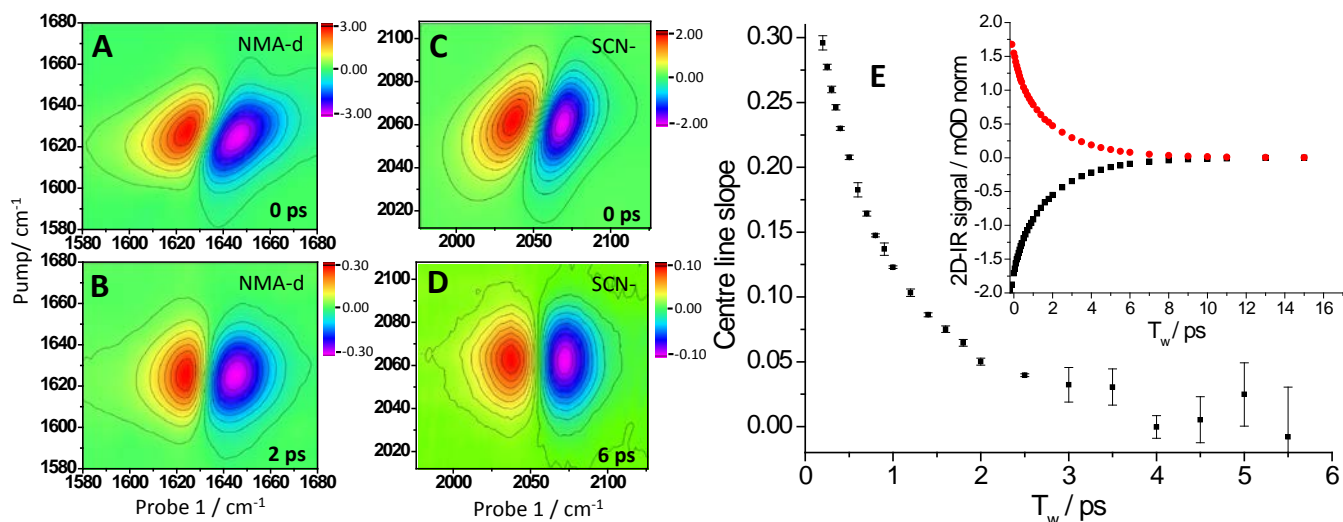

Fig. 3. Diagonal 2D-IR spectra. (a) and (b) The Amide I' band of NMA in dissolved in D_2O at 100 mM concentration, 0 and 2 ps waiting times respectively, 1s signal averaging time. (c) and (d) nitrile stretch NaSCN (100 mM) in H_2O, 0 and 6 ps waiting times respectively. (e) Centre-line slope fits to a waiting time series of nitrile stretch 2D-IR spectra. The inset shows the decay of the bleach and excited state absorption intensity for the data. The 2D-IR spectra scale bars are in units of mOD norm, as defined in the text.

2D-IR spectra II. Dual OPA probing. To demonstrate the utility of two independently tunable probe beams, and to further illustrate that the 80 cm⁻¹ pump bandwidth is adequate for practical 2D-IR spectroscopy, spectra of a sequence of DNA (10 mM, Adenine : Thymine, $(AT)_n$) and of Green Fluorescent Protein (GFP, ~15 mg/ml, chosen as the amide I band is characteristic of the protein's predominantly β-sheet composition). Both samples were dissolved in D_2O. Examples of their dual-probe 2D-IR spectra are shown in Figure 4. A full discussion of the interpretation of the DNA data can be found elsewhere.[38,39] For both the DNA and GFP, the pump is centered around 1650 cm⁻¹. In the case of DNA the pump excites base-pair carbonyl and ring modes. Probe 1 has been centred at 1060 cm⁻¹ to monitor the backbone modes (Figure 4(a)) and probe 2 has been set on-diagonal at 1650 cm⁻¹ to simultaneously monitor the base-pair

carbonyl and ring modes (Figure 4(b)). Four base-pair modes (two ring and two carbonyl) and their cross peaks are all clearly observed along the pump axis (Figure 4(b)) across a range of 100 cm^{-1}. Figure 4(a) shows the simultaneous measurement of the couplings of these modes to the DNA backbone modes. The GFP data shows simultaneous monitoring of the Amide I' diagonal and Amide I'-Amide II' cross peaks. An important property of the diagonal spectrum of the GFP is that the characteristic features of a β-sheet protein are clear in the shape of the spectrum,[40] again an indication that the bandwidth of the pump laser is sufficient for protein Amide I analysis – an important application of 2D-IR spectroscopy, where the bandshapes have been previously demonstrated as a good measure of protein secondary structure content.[7,41] Simultaneous monitoring of the Amide II' region holds promise as an enhanced form of secondary structure determination.
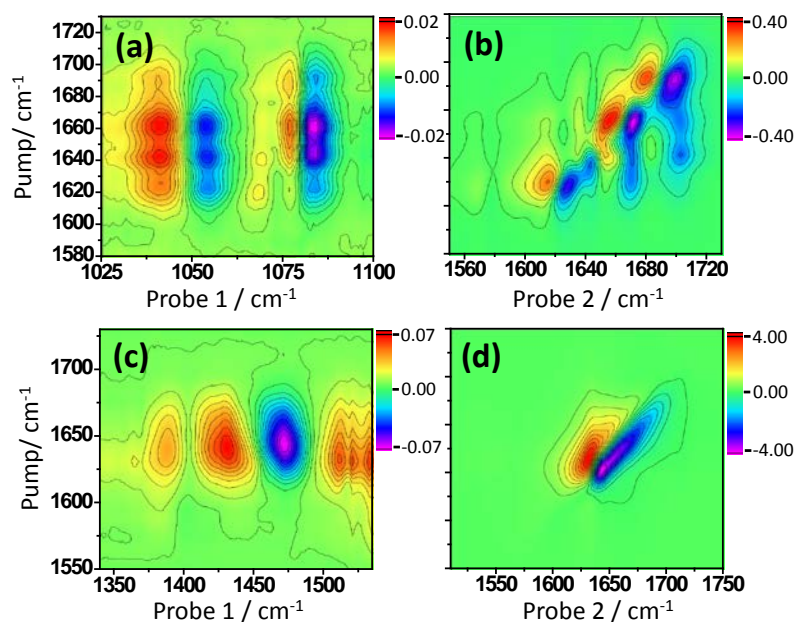

Fig. 4. Dual probe 2D-IR spectra of DNA ((AT)$_n$ n= 15, (a) and (b), see reference [38]) and GFP ((c) and (d)). The population time for both samples was 250 fs. (a) and (b) were recorded simultaneously with 1000s signal average. (c) and (d) were recorded simultaneously with a 10s signal average. The 2D-IR spectra scale bars are in units of mOD norm, as defined in the text.

2D-IR spectroscopy III. Sensitivity for weak signal acquisitions. The main motivation for using a 100 kHz system is to achieve a higher signal-to-noise. Such gains can be used to perform measurements faster, or to measure weak 2D-IR signals. For the former, we note that excellent quality NMA-d data such as that in Figure 3 was collected in 1 second. For strong carbonyl systems in general, 100 shots per coherence time point is often adequate for the strong signals observed. A pulse shaper acquisition of several-hundred waveforms would therefore take several milliseconds, which opens up very interesting possibilities for the sub-second 2D-IR monitoring of non-equilibrium chemical reactions. For the measurement of weak 2D-IR signals, Figure 5 shows an Amide I' 2D-IR spectrum of a ~300 nM solution of Myoglobin in D$_2$O, which for 154 residues corresponds to an equivalent concentration of ~50 µM Amide I groups in total. The acquisition time was 1000s, with a signal-to-noise of ~35 across the center (Figure 5 (b), the ratio of the peak-peak signal to the peak-peak noise).
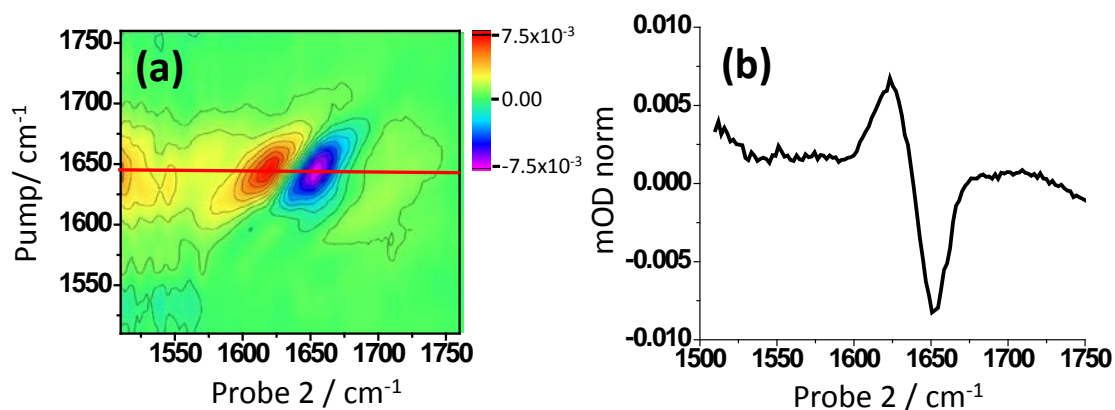
Fig. 5. (a) Amide I 2D-IR spectrum from 333 nM Myoglobin, 1000s average (b) a cut through the 2D-IR spectrum at ~1650 cm^{-1} illustrating signal-to-noise. The 2D-IR spectra scale bar are is in units of mOD norm, as defined in the text.

High average powers. Sample heating considerations. Although vibrational excitation of samples in 2D-IR experiments typically dissipates on sub-nanosecond timescales, a practical limit can be reached in high average power experiments due to equilibrium sample heating. In addition to average incident laser power, temperature rises depend on the optical density of the sample at the laser wavelengths and on the thickness, thermal conductivity and heat capacity of the solvent and windows. Heating effects are best quantified in a 2D-IR setup by measuring the differential absorbance of the (in this case weak) probe beam through the sample in the steady state with and without the pump beam present. This can then be compared with an infrared absorption spectrum of the same sample measured in a benchtop Fourier transform instrument using a temperature calibrated and heated sample cell. An example of such a measurement is shown in Figure 6 using 100 mM NaSCN dissolved in ethyl ammonium nitrate, an ionic liquid with 4x poorer thermal conductivity than water. The cell is 50 μm in pathlength and uses 2 mm CaF$_2$ windows. The pump is centred on the NaSCN band at 2050 cm^{-1} and roughly 50% of the shaped pump light was absorbed by the sample. The pulse shaper was operating using a 732-waveform pulse-pair phase and time scan (coherence time scanned to 4 ps in 22 fs steps), giving a pump power of 12 mW incident on the sample and a consequent increase in temperature of a few degrees, as evidenced by comparing the magnitude of the NaSCN bleaches at 2050 cm^{-1} in Figure 6. For H$_2$O / D$_2$O dissolved samples in the 50 μm pathlength CaF$_2$ cells commonly used, with 10-20 mW of shaped light incident on the sample we observe negligible heating, an important factor in work conducted with the 100 kHz instrument observing the melting of DNA as a function of temperature.[38] For volatile organic solvents with low thermal conductivity and low heat capacity, such as dichloromethane, 20-30 mW of focussed pump light is enough to cause thermal lensing, induce convection (causing instabilities in probe light transmission) and boiling. Under these conditions, rastering the sample over a 5 mm^2 area at 5-10 Hz can remove these effects.
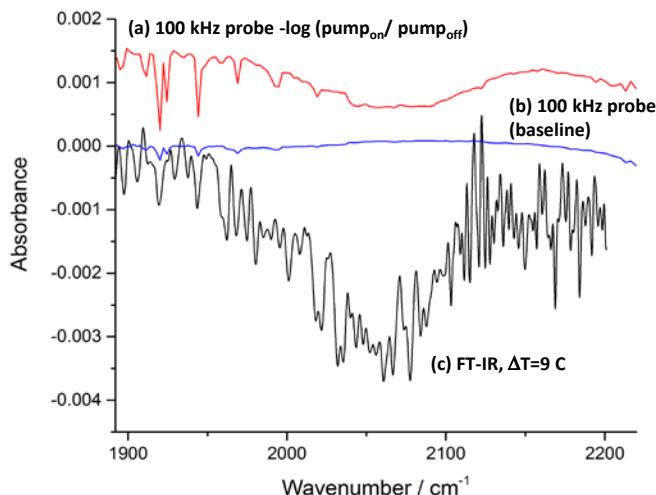
Fig. 6. An example measurement of the characterization of a sample's steady state temperature rise in the focus of the pulse-shaped 100 kHz pump beam via probe light transmission. The sample is 100 mM NaSCN dissolved in ethyl ammonium nitrate. (a) shows the absorbance change of the probe light when pumped. (b) shows an example baseline measurement (no pump light). 1 minute acquisition times were used for the measurements and we note that the offset of both (a) and (b) varied by +- 2 mOD due to laser intensity fluctuations between measurements. (c) shows the FT-IR measured absorbance change of the sample bought about by heating by 9 C above room temperature.

Conclusions

In conclusion, we have described and demonstrated a 100 kHz pulse shaping 2D-IR spectrometer based on Yb:KGW amplifiers. The speed at which data can be acquired, the flexibility of the three IR sources generating pump and two probe beams, the stability of the lasers and the compactness of the entire setup are a major step forward for 2D-IR spectroscopy. We observe an instrument response of 250 - 300 fs and by examining NaSCN in H_2O demonstrate that it is possible to accurately measure spectral diffusion close to these timescales timescales. By examining several other well-studied samples; NMA-d, DNA and a typical β-sheet protein, we have demonstrated that the narrower bandwidth of the Yb:KGW system does not limit its applicability in 2D-IR spectroscopy. In fact there are significant signal intensity advantages with narrower bandwidths if >100 cm^{-1} bandwidth pumping and < 300 fs dynamics can be sacrificed.

References

(1)   Hamm, P.; Zanni, M. T. *Concepts and methods in 2D infrared spectroscopy*; Cambridge, 2011.

(2)   Roberts, S. T.; Ramasesha, K.; Tokmakoff, A. *Structural rearrangements in water viewed through two-dimensional infrared spectroscopy, Accounts of Chemical Research* **2009**, *42*, 1239.

(3)   Thaemer, M.; De Marco, L.; Ramasesha, K.; Mandal, A.; Tokmakoff, A. *Ultrafast 2D IR spectroscopy of the excess proton in liquid water, Science* **2015**, *350*, 78.

(4)   Cahoon, J. F.; Sawyer, K. R.; Schlegel, J. P.; Harris, C. B. *Determining transition-state geometries in liquids using 2D-IR, Science* **2008**, *319*, 1820.

(5)   Zheng, J. R.; Kwak, K.; Asbury, J.; Chen, X.; Piletic, I. R.; Fayer, M. D. *Ultrafast dynamics of solute-solvent complexation observed at thermal equilibrium in real time, Science* **2005**, *309*, 1338.

(6)   Buchanan, L. E.*et al Mechanism of IAPP amyloid fibril formation involves an intermediate with a transient beta-sheet, Proceedings of the National Academy of Sciences of the United States of America* **2013**, *110*, 19285.

(7)   Baiz, C. R.; Peng, C. S.; Reppert, M. E.; Jones, K. C.; Tokmakoff, A. *Coherent two-dimensional infrared spectroscopy: Quantitative analysis of protein secondary structure in solution, Analyst* **2012**, *137*, 1793.

(8)   Bandaria, J. N.; Dutta, S.; Hill, S. E.; Kohen, A.; Cheatum, C. M. *Fast enzyme dynamics at the active site of formate dehydrogenase, J. Am. Chem. Soc.* **2008**, *130*, 22.

(9)   Adamczyk, K.*et al The effect of point mutation on the equilibrium structural fluctuations of ferric Myoglobin, Physical Chemistry Chemical Physics* **2012**, *14*, 7411.

(10) Hamm, P.; Lim, M. H.; Hochstrasser, R. M. *Structure of the amide I band of peptides measured by femtosecond nonlinear-infrared spectroscopy, Journal of Physical Chemistry B* **1998**, *102*, 6123.

(11) Shim, S.-H.; Strasfeld, D. B.; Ling, Y. L.; Zanni, M. T. *Automated 2D IR spectroscopy using a mid-IR pulse shaper and application of this technology to the human islet amyloid polypeptide, Proceedings of the National Academy of Sciences of the United States of America* **2007**, *104*, 14197.

(12) Helbing, J.; Hamm, P. *Compact implementation of Fourier transform two-dimensional IR spectroscopy without phase ambiguity, Journal of the Optical Society of America B-Optical Physics* **2011**, *28*, 171.

(13) Rehault, J.; Helbing, J. *Angle determination and scattering suppression in polarization-enhanced two-dimensional infrared spectroscopy in the pump-probe geometry, Optics express* **2012**, *20*, 21665.

(14) Rehault, J.; Maiuri, M.; Manzoni, C.; Brida, D.; Helbing, J.; Cerullo, G. *2D IR spectroscopy with phase-locked pulse pairs from a birefringent delay line, Optics express* **2014**, *22*, 9063.

(15) Anna, J. M.; Nee, M. J.; Baiz, C. R.; McCanne, R.; Kubarych, K. J. *Measuring absorptive two-dimensional infrared spectra using chirped-pulse upconversion detection, Journal of the Optical Society of America B-Optical Physics* **2010**, *27*, 382.

(16) Volkov, V.; Schanz, R.; Hamm, P. *Active phase stabilization in Fourier-transform two-dimensional infrared spectroscopy, Optics Letters* **2005**, *30*, 2010.

(17) Bloem, R.; Garrett-Roe, S.; Strzalka, H.; Hamm, P.; Donaldson, P. *Enhancing signal detection and completely eliminating scattering using quasi-phase-cycling in 2D IR experiments, Optics express* **2010**, *18*, 27067.

(18) Spector, I. C.; Olson, C. M.; Huber, C. J.; Massari, A. M. *Simple fully reflective method of scatter reduction in 2D-IR spectroscopy, Optics Letters* **2015**, *40*, 1850.

(19) Middleton, C. T.; Strasfeld, D. B.; Zanni, M. T. *Polarization shaping in the mid-IR and polarization-based balanced heterodyne detection with application to 2D IR spectroscopy, Optics express* **2009**, *17*, 14526.

(20) Nyby, C. M.; Leger, J. D.; Tang, J.; Varner, C.; Kireev, V. V.; Rubtsov, I. V. *Mid-IR beam direction stabilization scheme for vibrational spectroscopy, including dual-frequency 2DIR, Optics express* **2014**, *22*, 6801.

(21) Kanal, F.; Keiber, S.; Eck, R.; Brixner, T. *100-kHz shot-to-shot broadband data acquisition for high-repetition-rate pump-probe spectroscopy, Optics express* **2014**, *22*, 16965.

(22) Greetham, G. M.; Donaldson, P. M.; Nation, C.; Sazanovich, I. V.; Clark, I. P.; Shaw, D. J.; Parker, A. W.; Towrie, M. *100 kHz time-resolved multiple-probe femtoseconds to second IR absorption spectrometer*, *Appl. Spectrosc.* **2016**, *70*.

(23) Liebel, M.; Schnedermann, C.; Wende, T.; Kukura, P. *Principles and applications of broadband impulsive vibrational spectroscopy*, *J. Phys. Chem. A* **2015**, *119*, 9506.

(24) Kearns, N. M.; Mehlenbacher, R. D.; Jones, A. C.; Zanni, M. T. *Broadband 2D electronic spectrometer using white light and pulse shaping: noise and signal evaluation at 1 and 100 kHz*, *Optics express* **2017**, *25*, 7869.

(25) Son, M.; Mosquera-Vazquez, S.; Schlau-Cohen, G. S. *Ultrabroadband 2D electronic spectroscopy with high-speed, shot-to-shot detection*, *Optics express* **2017**, *25*, 18950.

(26) Luther, B. M.; Tracy, K. M.; Gerrity, M.; Brown, S.; Krummel, A. T. *2D IR spectroscopy at 100 kHz utilizing a mid-IR OPCPA laser source*, *Optics express* **2016**, *24*, 4417.

(27) Tracy, K. M.; Barich, M. V.; Carver, C. L.; Luther, B. M.; Krummel, A. T. *High-throughput two-dimensional infrared (2D IR) spectroscopy achieved by interfacing microfluidic technology with a high repetition rate 2D IR spectrometer*, *J. Phys. Chem. Lett.* **2016**, *7*, 4865.

(28) Thire, N.; Maksimenka, R.; Kiss, B.; Ferchaud, C.; Bizouard, P.; Cormier, E.; Osvay, K.; Forget, N. *4-W, 100-kHz, few-cycle mid-infrared source with sub-100-mrad carrier-envelope phase noise*, *Optics express* **2017**, *25*, 1505.

(29) Roberts, S. T.; Loparo, J. J.; Ramasesha, K.; Tokmakoff, A. *A fast-scanning Fourier transform 2D IR interferometer*, *Optics Communications* **2011**, *284*, 1062.

(30) Shim, S. H.; Strasfeld, D. B.; Fulmer, E. C.; Zanni, M. T. *Femtosecond pulse shaping directly in the mid-IR using acousto-optic modulation*, *Optics Letters* **2006**, *31*, 838.

(31) Hamm, P.; Kaindl, R. A.; Stenger, J. *Noise suppression in femtosecond mid-infrared light sources*, *Optics Letters* **2000**, *25*, 1798.

(32) Demirdoven, N.; Khalil, M.; Golonzka, O.; Tokmakoff, A. *Dispersion compensation with optical materials for compression of intense sub-100-fs mid-infrared pulses*, *Optics Letters* **2002**, *27*, 433.

(33) Nite, J. M.; Cyran, J. D.; Krummel, A. T. *Active Bragg angle compensation for shaping ultrafast mid-infrared pulses*, *Optics express* **2012**, *20*, 23912.

(34) Backus, E. H. G.; Garrett-Roe, S.; Hamm, P. *Phasing problem of heterodyne-detected two-dimensional infrared spectroscopy*, *Optics Letters* **2008**, *33*, 2665.

(35) Shaw, D. J.*et al* *Multidimensional infrared spectroscopy reveals the vibrational and solvation dynamics of isoniazid*, *J. Chem. Phys.* **2015**, *142*.

(36) Donaldson, P. M.; Hamm, P. *Gold nanoparticle capping layers: structure, dynamics, and surface enhancement measured using 2D-IR spectroscopy*, *Angewandte Chemie-International Edition* **2013**, *52*, 634.

(37) Czurlok, D.; von Domaros, M.; Thomas, M.; Gleim, J.; Lindner, J.; Kirchner, B.; Voehringer, P. *Femtosecond 2DIR spectroscopy of the nitrile stretching vibration of thiocyanate anions in liquid-to-supercritical heavy water. Spectral diffusion and libration-induced hydrogen-bond dynamics*, *Physical Chemistry Chemical Physics* **2015**, *17*, 29776.

(38) Hithell, G.; Shaw, D. J.; Donaldson, P. M.; Greetham, G. M.; Towrie, M.; Burley, G. A.; Parker, A. W.; Hunt, N. T. *Long-range vibrational dynamics are directed by Watson-Crick base pairing in duplex DNA*, *Journal of Physical Chemistry B* **2016**, *120*, 4009.

(39) Krummel, A. T.; Mukherjee, P.; Zanni, M. T. *Inter and intrastrand vibrational coupling in DNA studied with heterodyned 2D-IR spectroscopy*, *Journal of Physical Chemistry B* **2003**, *107*, 9165.

(40) Ghosh, A.; Ostrander, J. S.; Zanni, M. T. *Watching proteins wiggle: mapping structures with two dimensional infrared spectroscopy*, *Chemical Reviews* **2017**, *117*, 10726.

(41) Minnes, L.*et al* *Quantifying secondary structure changes in calmodulin using 2D-IR spectroscopy*, *Analytical chemistry* **2017**, *89*, 10898.

TOC GRAPHIC